

# A Sparse Sampling Approach to Dynamic Sub-Cycle Decomposition of Apparent Power in General Polyphase Networks

**Abstract.** We present a dynamic decomposition of apparent power in a polyphase network, based on measurements taken within a portion of a single cycle of the ac fundamental. We show that two time samples suffice for a definition that provides an attractive trade-off between computational cost and dynamic performance. The sub-cycle (or near-instantaneous) metrics that we introduce connect the time- and frequency-domain approaches in a natural way, and address the key weaknesses of the existing instantaneous decompositions. Furthermore, our power metrics are amenable to refinements via symmetrical components, thus connecting with concepts commonly used in system protection. We illustrate the sub-cycle decomposition via two polyphase examples: one of conceptual interest, the other an actual industrial voltage sag event.

**Streszczenie.** Przedstawiono dynamiczny rozkład mocy pozornej w obwodzie wielofazowym, oparty na pomiarach w części pojedynczego okresu harmonicznej podstawowej. Pokazano, że dwie próbki wystarczają dla definicji, która jest atrakcyjnym kompromisem pomiędzy kosztem obliczeniowym a zachowaniem dynamicznym. Wprowadzone pod-okresowe (lub niemal-chwilowe) macierze, łączą podejście w dziedzinie czasowej z podejściem częstotliwościowym naturalny i dotyczą kluczowej słabości istniejących rozkładów chwilowych. Ponadto, wprowadzone macierze mocy są podatne na uproszczenia z pomocą składowych symetrycznych, nawiązując w ten sposób do metod powszechnie stosowanych w technice zabezpieczeniowej. Rozkład pod-okresowy ilustrowany jest dwoma przykładami wielofazowymi: jeden o charakterze poznawczym i drugi dotyczący przemysłowej zapaści napięcia. (Dynamiczny Rozkład Mocy Pozornej Metoda Rzadkiego Próbkowania w Pod-Okresie ()

**Keywords:** Apparent Power, Reactive Power, Polyphase Networks, Time-Domain, Time Varying Systems

**Słowa kluczowe:** Moc pozorna, obwody wielofazowe, dziedzina czasowa, dziedzina częstotliwości, systemy zmienne w czasie.

## Introduction

The importance of AC devices and systems in all areas of electric energy generation, transmission and conversion naturally raises questions about characterization of their operating regimes. With the persistent increase in control bandwidths brought about by the power electronics, it has become important to develop fast-varying metrics that can capture both transient and steady-state behavior.

In this paper we aim to address some of the weaknesses of commonly used concepts of instantaneous reactive power. The instantaneous facet (single sample, possibly vector in the case of polyphase systems) has the weakness of insufficient information [1]. For example, even a sinusoid of known frequency requires two parameters for a complete characterization (e.g., magnitude and phase), and the two can not be resolved from a single data point. Thus, for example, the standard instantaneous reactive power [2] can not be defined for single phase systems. In the case of vector measurements, there is more information present, but a polyphase system requires more parameter estimates in general (i.e., without simplifying assumptions like balancedness and known frequency content). The other key weakness is that in the case of general polyphase systems there exist more than one scalar instantaneous reactive power, which can best be seen from representation-free descriptions, like the ones based on geometric algebra [3].

We are interested in solutions that are based on a few samples (hence the “sparse sampling” label) and in solutions that do not require a full cycle (or period) record of the AC waveform. It will turn out that the class of solutions that we propose bridges the time and frequency domains in the sense that we use as few as only two samples in the time domain, but our sampling policy is informed by knowledge of the fundamental frequency of the AC waveform.

The concept that we advance in this paper has connections with approaches based on derivatives or integrals of currents and voltages that have been described in papers such as [4, 5, 6]. This can be seen most directly in the case of a sinusoidal waveform, where a quarter-period time-shift corresponds to a (signed) derivative or integral.

By using a small number of time-domain samples

we also bridge the gap between the purely-instantaneous (single-sample) power metrics of [2] and the 7/11-component dynamic decomposition of [7], which relies on a full-cycle (sliding-window) record of voltage and current waveforms. Thus, the approach we propose here provides a flexible trade-off between computational cost, which increases with the number of time-domain samples used, and the attendant improvement in quality of the resulting dynamic power metrics.

We demonstrate in this paper that a very significant improvement in the quality of dynamic power metrics, as compared with the purely-instantaneous metrics of [2], can be achieved by using just two time-domain samples of the (polyphase) voltage and current waveforms. The information contained in two samples of any  $m$ -phase waveform allows us to construct a dynamic  $m$ -phase complex phasor, resulting in a one-to-one correspondence between the time and frequency domains (see eq. (1) below). The constructed (polyphase) voltage and current phasors are then used to obtain a dynamic 4-component decomposition of apparent power. In addition, we are also able to decompose our dynamic sub-cycle real and reactive power metrics into their symmetrical sequence components.

## Sub-Cycle Dynamic Phasors

Given any polyphase (row-vector) waveform  $x(t)$  we define a Sub-Cycle (or near-instantaneous) dynamic phasor  $\hat{X}_1(t)$ , viz.,

$$(1) \quad \hat{X}_1(t) \stackrel{\text{def}}{=} \frac{1}{\sqrt{2}} e^{-j\omega t} \left[ x(t) + jx(t - \frac{T}{4}) \right]$$

where  $\omega = 2\pi/T$  denotes the steady state fundamental frequency. Observe that, as a consequence of (1)

$$x(t) = \sqrt{2} \Re \left\{ \hat{X}_1(t) e^{j\omega t} \right\}$$

as well as

$$\begin{aligned}\|\widehat{X}_1(t)\|^2 &\stackrel{\text{def}}{=} \widehat{X}_1(t) \widehat{X}_1^H(t) \\ &= \frac{1}{2} \left[ x(t) x^T(t) + x(t - \frac{T}{4}) x^T(t - \frac{T}{4}) \right] \\ &\stackrel{\text{def}}{=} X_{rms}^2(t)\end{aligned}$$

We can now apply these concepts to any given pair of polyphase voltage and current waveforms, resulting in an associated sub-cycle dynamic voltage phasor  $\widehat{V}_1(t)$  and a sub-cycle dynamic current phasor  $\widehat{I}_1(t)$ . In addition to the rms relations

$$\begin{aligned}V_{rms}^2(t) &\stackrel{\text{def}}{=} \|\widehat{V}_1(t)\|^2 \\ &= \frac{1}{2} \left[ v(t) v^T(t) + v(t - \frac{T}{4}) v^T(t - \frac{T}{4}) \right] \\ I_{rms}^2(t) &\stackrel{\text{def}}{=} \|\widehat{I}_1(t)\|^2 \\ &= \frac{1}{2} \left[ i(t) i^T(t) + i(t - \frac{T}{4}) i^T(t - \frac{T}{4}) \right]\end{aligned}$$

we can also define sub-cycle real and reactive power, viz.,

$$\begin{aligned}(3) \quad P(t) &\stackrel{\text{def}}{=} \Re \left\{ \widehat{V}_1(t) \widehat{I}_1^H(t) \right\} \\ Q(t) &\stackrel{\text{def}}{=} \Im \left\{ \widehat{V}_1(t) \widehat{I}_1^H(t) \right\}\end{aligned}$$

and observe that

$$(4a) \quad P(t) = \frac{1}{2} \left[ v(t) i^T(t) + v(t - \frac{T}{4}) i^T(t - \frac{T}{4}) \right]$$

Thus our sub-cycle real power is a 2-sample average of the instantaneous power  $p(t) \stackrel{\text{def}}{=} v(t) i^T(t)$ , namely

$$(4b) \quad P(t) = \frac{1}{2} \left[ p(t) + p(t - \frac{T}{4}) \right]$$

The 2-sample averaging operation removes fluctuations of  $p(t)$  caused by the fundamental harmonic of the voltage and current.

Similarly, we observe that

$$(5) \quad \begin{aligned}Q(t) &= \frac{1}{2} \left[ v(t - \frac{T}{4}) i^T(t) - v(t) i^T(t - \frac{T}{4}) \right] \\ &= \frac{1}{2} \left[ v(t) v(t - \frac{T}{4}) \right] \begin{pmatrix} 0 & -1 \\ 1 & 0 \end{pmatrix} \begin{pmatrix} i(t) & i(t - \frac{T}{4}) \end{pmatrix}^T\end{aligned}$$

### Sub-Cycle Four-Component Decomposition of Apparent Power

The sub-cycle apparent power is defined as

$$(6) \quad S(t) \stackrel{\text{def}}{=} V_{rms}(t) I_{rms}(t) \equiv \|\widehat{V}_1(t)\| \|\widehat{I}_1(t)\|$$

and it follows from the Cauchy-Schwarz inequality that

$$\begin{aligned}S^2(t) - [P^2(t) + Q^2(t)] &\equiv \\ \|\widehat{V}_1(t)\|^2 \|\widehat{I}_1(t)\|^2 - \|\widehat{V}_1(t) \widehat{I}_1^H(t)\|^2 &\geq 0\end{aligned}$$

This gap can be decomposed into a sum of (squares of) two components that describe the load imbalance among

phases. To this end, define an equivalent polyphase admittance

$$(7) \quad G(t) - jB(t) \stackrel{\text{def}}{=} \frac{\widehat{I}_1(t)}{\widehat{V}_1(t)}$$

where the ratio of two (row) vectors is defined in terms of element-wise division (same as  $\widehat{I}_1(t)/\widehat{V}_1(t)$ ) in MATLAB). The gap  $S^2(t) - [P^2(t) + Q^2(t)]$  is directly related to the fact that the elements of  $G(t) - jB(t)$  are not necessarily equal to each other.

Borrowing from the theory of statistics, we now introduce the *weighted mean* operation  $\mathcal{M}_w$  for any (row) vector  $X = \{x_k\}$ , viz.,

$$(8) \quad \mathcal{M}_w X \stackrel{\text{def}}{=} \sum_k w_k x_k$$

where the real-valued, non-negative coefficients  $w_k$  serve as (relative) weights, and  $\sum_k w_k = 1$ .

To capture the variation (across phases) of the elements of  $G(t)$  and  $B(t)$ , we define the time-varying weights

$$(9) \quad w_k(t) \stackrel{\text{def}}{=} \frac{1}{V_{rms}^2(t)} \left| \widehat{V}_1^{(k)}(t) \right|^2$$

and observe that, as a result of our definition of  $\mathcal{M}_w$ ,

$$\begin{aligned}(10) \quad \mu_g(t) &\stackrel{\text{def}}{=} \mathcal{M}_w G(t) = \frac{P(t)}{V_{rms}^2(t)} \\ \mu_b(t) &\stackrel{\text{def}}{=} \mathcal{M}_w B(t) = \frac{Q(t)}{V_{rms}^2(t)}\end{aligned}$$

Notice that in our case the weighted mean  $\mathcal{M}_w$  is a time-variant operator, since it uses a set of time-varying weights. A well-known result from statistics [8] states that for any (row) vector  $X$

$$(11) \quad \mathcal{M}_w X^2 = \mathcal{M}_w \left( X - \mu_x \mathbf{1} \right)^2 + \mu_x^2$$

where  $\mu_x \stackrel{\text{def}}{=} \mathcal{M}_w X$  is the mean value of the elements of  $X$ . Here  $\mathbf{1} \stackrel{\text{def}}{=} [\underbrace{1 \ 1 \ \cdots \ 1}_m]$ , where  $m$  is the length of the vector  $X$ , and  $X^2$  denotes element-wise squaring of  $X$  (same as  $X \wedge 2$  in MATLAB).

We can also define

$$\begin{aligned}(12) \quad \sigma_g^2(t) &\stackrel{\text{def}}{=} \mathcal{M}_w \left( G(t) - \mu_g(t) \mathbf{1} \right)^2 \\ \sigma_b^2(t) &\stackrel{\text{def}}{=} \mathcal{M}_w \left( B(t) - \mu_b(t) \mathbf{1} \right)^2\end{aligned}$$

so that

$$(13) \quad \begin{aligned}\mathcal{M}_w G^2(t) &= \mu_g^2(t) + \sigma_g^2(t) \\ \mathcal{M}_w B^2(t) &= \mu_b^2(t) + \sigma_b^2(t)\end{aligned}$$

The definition of  $G(t) - jB(t)$  implies that

$$\left\| \widehat{I}_1(t) \right\|^2 = V_{rms}^2 \left[ \mathcal{M}_w G^2(t) + \mathcal{M}_w B^2(t) \right]$$

and, consequently,

$$\begin{aligned}(14) \quad S^2(t) &= V_{rms}^4 \left[ \mu_g^2(t) + \sigma_g^2(t) + \mu_b^2(t) + \sigma_b^2(t) \right] \\ &= P^2(t) + N_g^2(t) + Q^2(t) + N_b^2(t)\end{aligned}$$

where we define

$$(15a) \quad \begin{aligned} N_g(t) &\stackrel{\text{def}}{=} \sigma_g(t) V_{rms}^2(t) \\ N_b(t) &\stackrel{\text{def}}{=} \sigma_b(t) V_{rms}^2(t) \end{aligned}$$

and recall that

$$(15b) \quad \begin{aligned} P(t) &= \mu_g(t) V_{rms}^2(t) \\ Q(t) &= \mu_b(t) V_{rms}^2(t) \end{aligned}$$

In summary, the introduction of the sub-cycle dynamic phasors makes it possible to construct the 4-component decomposition (14) of the sub-cycle apparent power  $S(t)$ .

### Examples

**Example 1: RLC load** – consider a three phase system, driven by balanced fundamental and fifth harmonic voltages, with magnitudes 1 and 0.1, respectively. The load consists of a resistor in phase “a”, an inductor in phase “b”, and a capacitor in phase “c”, each drawing a unit magnitude current at the fundamental harmonic. The corresponding voltage and current phasors are summarized in Table 1.

Table 1. Voltage and current phasors

	a	b	c	
$V_1^{(p)}$	1	$e^{-j2\pi/3}$	$e^{j2\pi/3}$	
$V_5^{(p)}$	0.1	$0.1e^{-j2\pi/3}$	$0.1e^{j2\pi/3}$	
$I_1^{(p)}$	1	$e^{j5\pi/6}$	$e^{-j5\pi/6}$	
$I_5^{(p)}$	0.1	$0.02e^{j5\pi/6}$	$0.5e^{-j5\pi/6}$	

The sub-cycle power components  $P(t)$ ,  $Q(t)$ ,  $N_g(t)$ ,  $N_b(t)$  for this example are shown in Fig. 1 (solid red line). For comparison, we include also the instantaneous (Akagi-Nabae)  $p(t)$  and  $q(t)$ , shown by dashed line in Fig. 1. Notice that most of the fluctuation in  $p(t)$  and  $q(t)$  is eliminated by our 2-sample averaging technique. In fact, it can be shown that when the 5-th harmonic component is absent from the voltage and current waveforms, our four sub-cycle components become time-invariant (see solid red line in Fig 2). In contrast, the instantaneous  $p(t)$  and  $q(t)$  – shown by the dashed line in Fig 2 – still fluctuate with (essentially) the same range of values as in Fig 1.

Moreover, the *cycle-averaged values* of the sub-cycle  $P(t)$  and  $Q(t)$  of Fig. 1 coincide with the values obtained from the full-cycle 7/11-component decomposition of [7] (shown in Table 2). The sliding-cycle averages of the sub-cycle  $N_g(t)$ ,  $N_b(t)$  of Fig. 1 are also close to the full-cycle  $N_g$ ,  $N_b$  values of Table 2.

Table 2. Non-vanishing 7/11-components of apparent power

S	P	$Q_B$	$N_g$	$N_b$
3.1431	1.0100	-0.0480	1.4284	2.6108

**Example 2: industrial voltage sag event** – we now consider a set of data recorded in a paper plant during an outage described in [9] (the data was graciously provided to us by the authors).

The four sub-cycle power components are shown in Fig. 3 (solid red line), with the instantaneous  $p(t)$  and  $q(t)$  indicated by a blue dashed line. Again we notice drastic reduction of the fluctuations in  $p(t)$ ,  $q(t)$  achieved by our 2-sample averaging. Notice that in this example the plots use

a scale factor of  $10^{-3}$ , so that  $P(t)$  is in [kW],  $Q(t)$  is in [kVar], and  $N_g(t)$ ,  $N_b(t)$  are in [kVA].

These results should be compared with the (much smoother) dynamic real and reactive (Budeanu) power obtained from the full-cycle 7/11-component decomposition (Fig. 4, top two plots). Notice that  $P(t)$  and  $Q(t)$  of Fig. 3 fluctuate almost exactly around the values shown in Fig. 4. In contrast, the sub-cycle  $N_g(t)$  and  $N_b(t)$  differ significantly from their full-cycle counterparts in Fig. 4. A better match can be achieved by increasing the number of samples used (e.g., to 4 samples).

### Symmetrical Sequence Components for the Sub-Cycle $P(t)$ , $Q(t)$

Symmetrical power components (of the full-cycle real power  $P$ ) are a standard way to describe unbalanced operation and faults in three-phase systems [10]. We propose here to apply a similar split for the sub-cycle  $P(t)$  and  $Q(t)$  of (3).

The symmetrical sequence components of the dynamic phasors  $\hat{V}_1(t)$  and  $\hat{I}_1(t)$  in a 3-phase system are obtained by applying the unitary transformation

$$(16a) \quad \begin{aligned} [\hat{V}_0(t) &\quad \hat{V}_+(t) &\quad \hat{V}_-(t)] \stackrel{\text{def}}{=} \hat{V}_1(t) \mathcal{W} \\ [\hat{I}_0(t) &\quad \hat{I}_+(t) &\quad \hat{I}_-(t)] \stackrel{\text{def}}{=} \hat{I}_1(t) \mathcal{W} \end{aligned}$$

Here the subscript “0” denotes the zero sequence component, while the subscripts “+” and “-” denote the positive and negative sequence components, respectively. The unitary  $3 \times 3$  matrix  $\mathcal{W}$  is a (normalized) 3-point DFT matrix, viz.,

$$(16b) \quad \mathcal{W} = \frac{1}{\sqrt{3}} \begin{pmatrix} 1 & 1 & 1 \\ 1 & \alpha^* & \alpha \\ 1 & \alpha & \alpha^* \end{pmatrix}, \quad \alpha \stackrel{\text{def}}{=} e^{j2\pi/3}$$

Next we can express the quantity  $\hat{V}_1(t) \hat{I}_1(t)^H$ , used to determine both  $P(t)$  and  $Q(t)$ , in terms of the voltage and current symmetrical sequence phasors, viz.,

$$\hat{V}_1(t) \hat{I}_1(t)^H = [\hat{V}_0(t) \quad \hat{V}_+(t) \quad \hat{V}_-(t)] [\hat{I}_0(t) \quad \hat{I}_+(t) \quad \hat{I}_-(t)]^H$$

where we used the property  $\mathcal{W} \mathcal{W}^H = I$ . Splitting this expression into contributions from individual sequence components, we obtain additive decompositions for  $P(t)$  and  $Q(t)$ , viz.,

$$(17a) \quad \begin{aligned} P(t) &= P_0(t) + P_+(t) + P_-(t) \\ Q(t) &= Q_0(t) + Q_+(t) + Q_-(t) \end{aligned}$$

where

$$(17b) \quad \begin{aligned} P_0(t) &= \Re \{ \hat{V}_0(t) \hat{I}_0^H(t) \} \\ P_+(t) &= \Re \{ \hat{V}_+(t) \hat{I}_+^H(t) \} \\ P_-(t) &= \Re \{ \hat{V}_-(t) \hat{I}_-^H(t) \} \end{aligned}$$

and

$$(17c) \quad \begin{aligned} Q_0(t) &= \Im \{ \hat{V}_0(t) \hat{I}_0^H(t) \} \\ Q_+(t) &= \Im \{ \hat{V}_+(t) \hat{I}_+^H(t) \} \\ Q_-(t) &= \Im \{ \hat{V}_-(t) \hat{I}_-^H(t) \} \end{aligned}$$

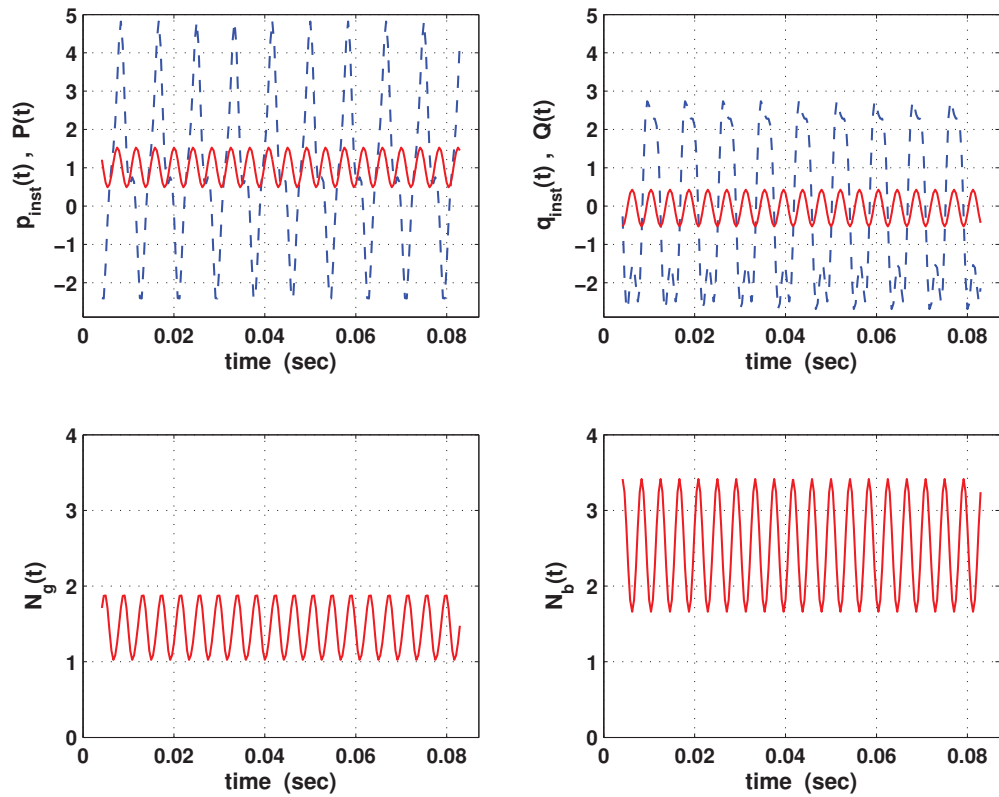


Fig. 1. **Example 1** (with 1st and 5th harmonics): sub-cycle power components (solid red line) vs. instantaneous power components (dashed blue line).

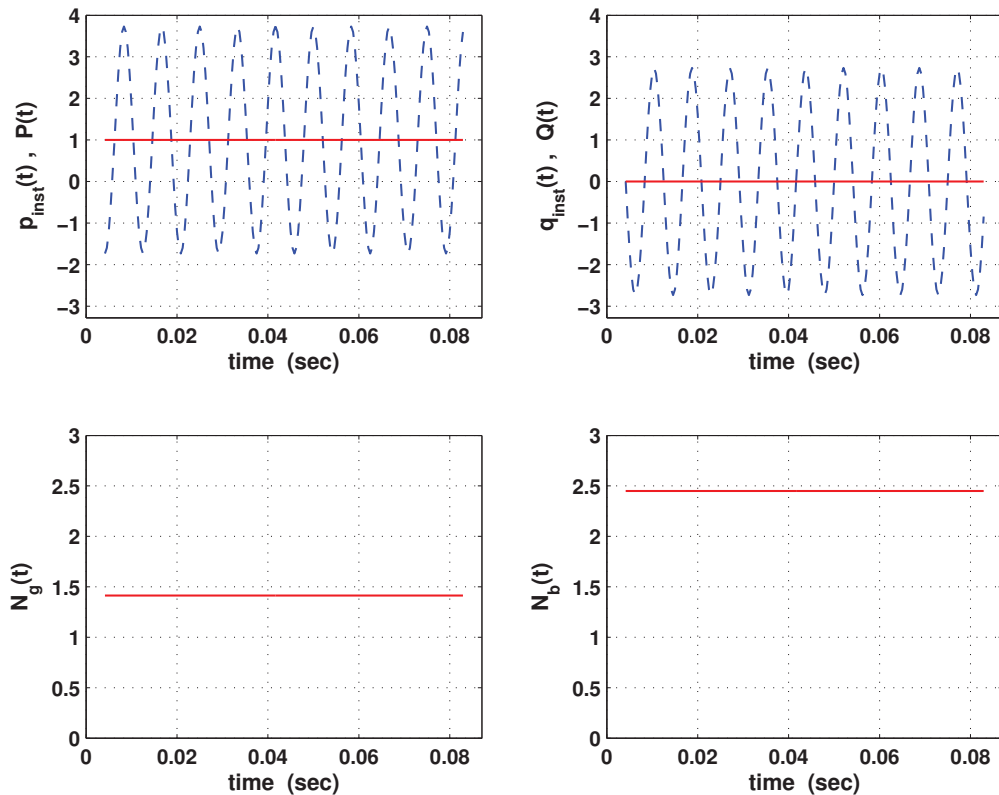


Fig. 2. **Example 1** (with 1st harmonic only): sub-cycle power components (solid red line) vs. instantaneous power components (dashed blue line).

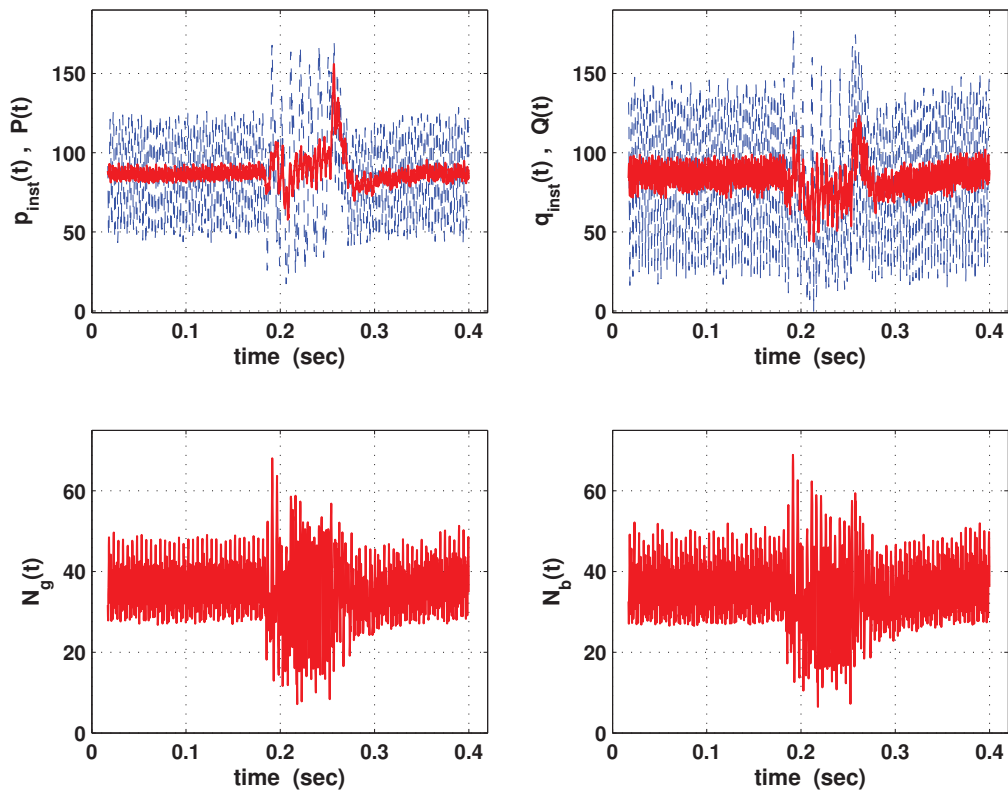


Fig. 3. **Example 2:** sub-cycle power components (solid red line) vs. instantaneous power components (dashed blue line).

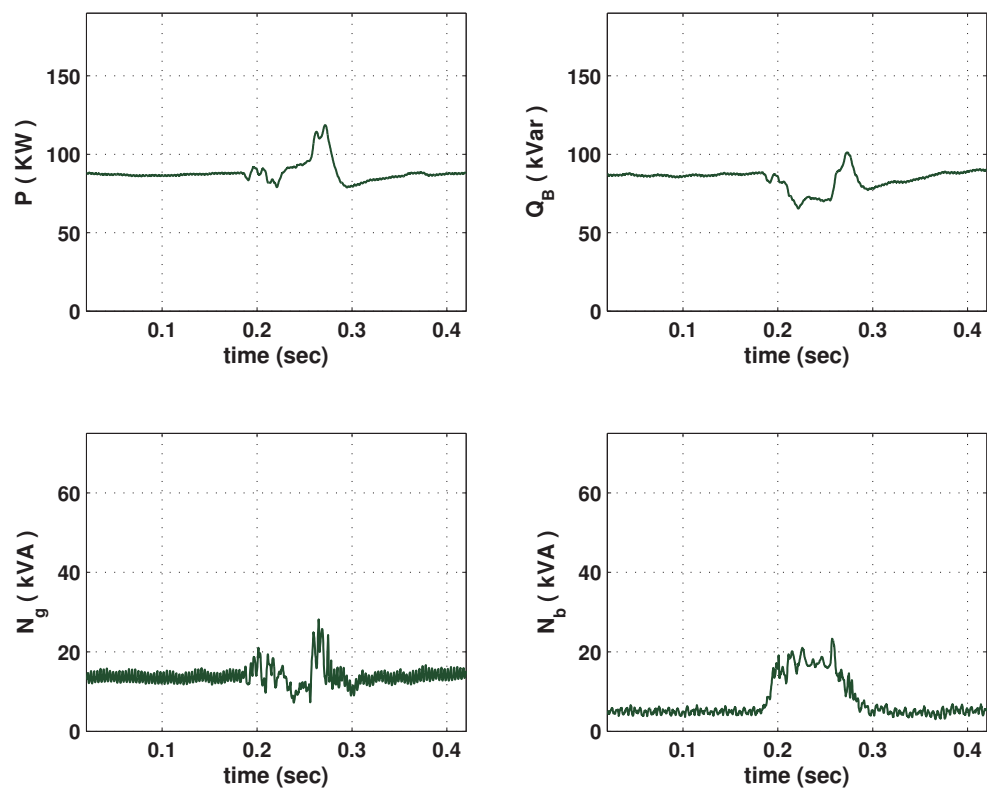


Fig. 4. **Example 2:** non-vanishing 7/11 power components (solid green line).

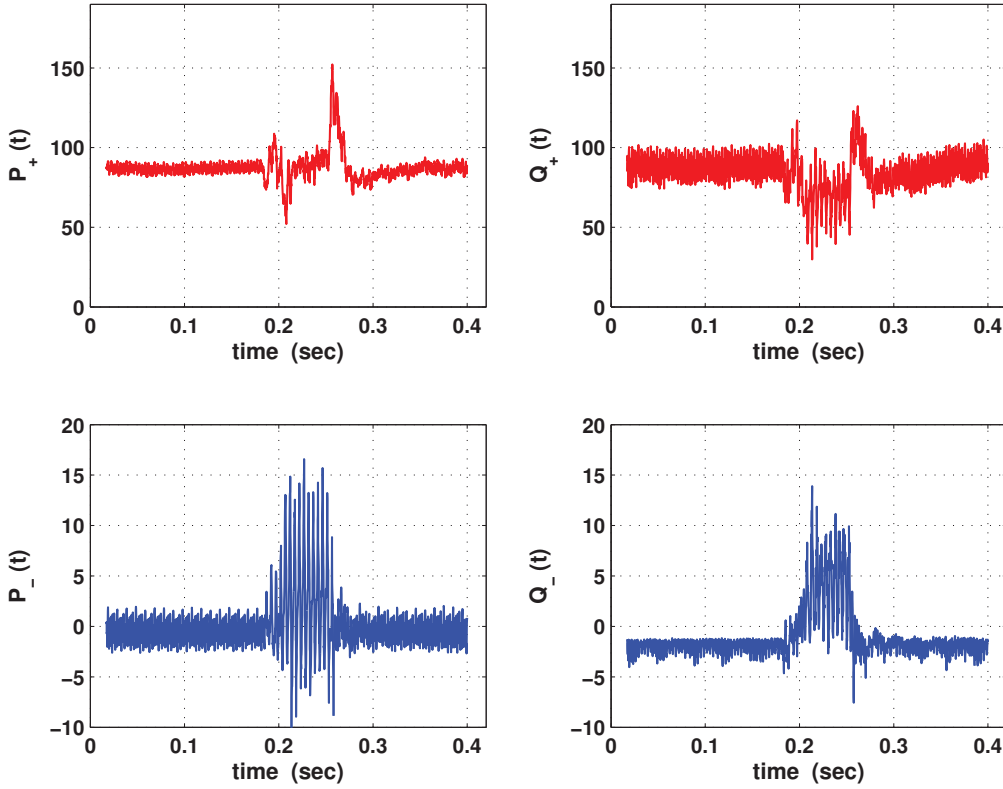


Fig. 5. **Example 2:** sub-cycle symmetrical sequence components of  $P(t)$  and  $Q(t)$ .

This means that the 4-component decomposition (14) consists, in fact, of eight components, viz.,

$$(17d) \quad S^2(t) = (P_+(t) + P_-(t) + P_0(t))^2 + N_g^2(t) + (Q_+(t) + Q_-(t) + Q_0(t))^2 + N_b^2(t)$$

The positive and negative sequence components of  $P(t)$  and  $Q(t)$  are shown in Fig. 5: the zero sequence components are negligible in this case. Notice that both  $P_-(t)$  and  $Q_-(t)$  provide an indication of the event duration (between 0.18 sec and 0.27 sec). Similar observations were made in [7] about the full-cycle counterparts of these negative sequence components.

### Concluding Remarks

We constructed a dynamic decomposition of apparent power in a polyphase network, that uses two samples separated by a quarter cycle. The resulting power metrics offer an attractive trade-off between performance and cost: they exhibit significantly smaller temporal fluctuation than the standard (Akagi) instantaneous real and reactive power metrics, while requiring only a modest increase in computational effort. Our dynamic decomposition uses only a single (polyphase) phasor for each waveform, in contrast to full-cycle power metrics (such as those of [1, 7]), which require a complete Fourier series representation.

The temporal fluctuation of our dynamic sub-cycle metrics when applied in a periodic (steady-state) setting depends on the harmonic content of the voltage and current waveforms, and decreases when more samples per cycle are used. For instance, increasing the number of samples per cycle from 2 to 4 results in non-fluctuating dynamic power components for our (steady-state) Example 1. Moreover, the values of the resulting sub-cycle  $P(t)$ ,  $Q(t)$ ,  $N_g(t)$  and  $N_b(t)$  for this example coincide with the full-cycle values of Table 2.

Our construction of dynamic sub-cycle power metrics relies on knowledge of the cycle length  $T$ . In practice, this quantity (like any estimated parameter) can only be known with finite precision. This means that the time-domain expression (4b) for  $P(t)$  is replaced by

$$P(t) = \frac{1}{2} [p(t) + p(t - \Delta)]$$

where  $\Delta = \frac{T}{4}(1 + \varepsilon)$ , and  $\varepsilon$  represents the relative error in  $T$ . Nevertheless, the local (sliding window) average of  $P(t)$  is essentially unaffected by the value of  $\varepsilon$  for periodic voltages and currents, and the same holds even in the presence of slow transients. The primary impact of the cycle-length error is on the temporal fluctuation of  $P(t)$  around its local average, and this effect increases monotonically with the magnitude of  $\varepsilon$ . In particular, it can be shown that the relative error in  $P(t)$ ,  $Q(t)$  for sinusoidal voltages and currents is (approximately) proportional to  $\varepsilon$ .

### REFERENCES

- [1] L.S. Czarnecki, "Meta-theory of electric powers and present state of power theory of circuits with periodic voltages and currents", *Przegląd Elektrotechniczny*, Vol. 89, No. 6, pp. 26-31, 2013.
- [2] H. Akagi, Y. Kanazawa and A. Nabae, "Instantaneous Reactive Power Compensators Comprising Switching Devices without Energy Storage Components", *IEEE Trans. Ind. Applic.*, Vol. 20, No.3, pp. 625-630, 1984.
- [3] H. Lev-Ari and A.M. Stankovic, "Instantaneous Power Quantities in Polyphase Systems - A Geometric Algebra Approach", *2009 IEEE Energy Conversion Conference and Exposition*, San Jose, CA, Sept. 2009.
- [4] M. Iliovici, "Definition et mesure de la puissance et de l'énergie réactives," *Bull. Soc. Franc. Electr.*, no. 5, pp. 931-954, 1925.
- [5] J. Wyatt and M. Ilić, "Time-Domain Reactive Power Concepts for Nonlinear, Nonsinusoidal or Nonperiodic Network," *IEEE Int'l. Symp. Circuits and Systems*, Volume 1, Issue 3, May 1990, pp. 387-390.
- [6] P. Tenti, P. Mattavelli, "A Time-domain Approach to Power Terms Definitions under Non-sinusoidal Conditions," *6th Int. Workshop*

- on Power Definitions and Measurement under Non-Sinusoidal Conditions*, Milan, Italy, 2003.
- [7] H. Lev-Ari, A.M. Stanković and A. Ghanavati, "Dynamic Decomposition of Apparent Power in Polyphase Unbalanced Networks with Application to Transients in an Industrial Load," *40-th North American Power Symposium*, Calgary, Canada, Sept. 2008.
  - [8] S.J. Orfanidis, *Optimum Signal Processing*, 2nd ed. McGraw-Hill, 1988.
  - [9] M. Radmehr, S. Farhangi and A. Nasiri, "The Power of Paper," *IEEE Industry Applications Magazine*, Sept./Oct. 2007, pp. 38-48.
  - [10] J.D. Glover, M.S. Sarma and T.J. Overbye, *Power System Analysis and Design*, 5th edition, Cengage Learning, 2012.

---

**Authors:** Prof. Hanoch Lev-Ari, Department of Electrical and Computer Engineering, Northeastern University, Boston, MA 02114, USA, email: [levari@ece.neu.edu](mailto:levari@ece.neu.edu), Prof. Aleksandar Stankovic, Department of Electrical and Computer Engineering, Tufts University, Medford, MA 02155, USA, email: [astankov@ece.tufts.edu](mailto:astankov@ece.tufts.edu).